Clays and Clay Minerals, Vol. 52, No. 5, 603–612, 2004.

Na BIOTITE AND INTERMEDIATE Na-K BIOTITE IN SCHISTS FROM THE BETIC CORDILLERAS (SPAIN)

MARÍA DOLORES RUIZ CRUZ*

Departamento de Química Inorgánica, Cristalografía y Mineralogía, Facultad de Ciencias, Universidad de Málaga, 29071 Málaga, Spain

Abstract—Submicroscopic intergrowths of K biotite, Na biotite and intermediate Na-K biotite from a schist near Málaga (Betic Cordilleras, Spain) were discovered using high-resolution transmission electron microscopy and analytical electron microscopy. The sample was also studied with X-ray diffraction, electron microprobe analysis, and scanning electron microscopy. Scanning electron microscopy revealed that the Na-enriched biotite is concentrated in albite-rich microdomains, albite being partially replaced by biotite. These images also revealed that both K and Na-K biotite grains appear locally retrograded to kaolinite. Transmission electron microscopic data indicated that K biotite, Na biotite and Na-K biotite form parallel or subparallel packets with interfaces parallel to the basal planes of biotite. Potassium biotite forms thick packets, chemically homogeneous, with a basal spacing of 10.1 Å. Sodium biotite also occurs as chemically homogeneous stacks of layers with a 9.78 Å periodicity. Sodium-K biotite shows, on the contrary, variable composition and basal spacings intermediate between K and Na biotites. Analytical electron microscopic data revealed important chemical differences between Na and K biotites, which affect both the tetrahedral and the octahedral sheets. Both electron microprobe analysis and analytical electron microscopy indicated that the trioctahedral micas show relatively low interlayer occupancy, suggesting the presence of H_3O^+ replacing the interlayer cations. Partial hydration of biotite explains the presence of a weak 14 Å reflection in the X-ray patterns. Both chemical and textural data suggested that these trioctahedral micas grew during a common prograde metamorphic episode, the phases with intermediate composition probably being metastable.

Key Words—Betic Cordilleras, EMPA, Na biotite, K biotite, SEM, TEM/AEM, Vermiculite, XRD.

INTRODUCTION

Natural biotites are predominantly potassic trioctahedral micas with only limited substitution by Na (Deer *et al*., 1976; Guidotti, 1984). Indeed, reports of naturally occurring Na-rich trioctahedral micas are scarce, and most of these deal with Na-Mg micas (Na phlogopite, wonesite and preiswerkite), which were first described in a few rather unusual host lithologies, such as Na-rich metadolomites (Schreyer *et al*., 1980), Ca-poor metavolcanics (Spear *et al*., 1981), and metarodingite (Keusen and Peters, 1980). In recent years, the number of reports of Na trioctahedral micas has gradually increased. Most of the Na phlogopites occur as inclusions in anhydrous phases (garnets and chromite) from ophiolitic sequences, where Na phlogopite coexists with pargasite (*e.g*. Peng *et al*., 1995; Cabella *et al*., 1997; Melcher *et al*., 1997; Yang and Jahn, 2000). On the other hand, most of the occurrences of preiswerkite have in common a polymetamorphic history involving retrogression of high-pressure rocks (*e.g*. Meyer, 1983; Smith, 1988; Godard and Smith, 1999).

Sodium biotites are also rare minerals that have been described in pelitic schists of the amphibolite facies (Dempster and Jackson, 1996) and metadikes from the Maláguide Complex (Ruiz Cruz and Novak, 2003). The low Na content in natural biotite (of the order of 0.05 atoms per 11 oxygens) (Deer *et al*., 1976; Guidotti, 1984) and the relatively low K content in natural Na phlogopite (up to 0.12 atoms per 11 oxygens) (Schreyer *et al*., 1980) suggest the existence of a wide miscibility gap in the system Na-K trioctahedral micas. Nevertheless, higher K contents have been found in wonesite (Spear *et al*., 1981) and in Na biotite (Dempster and Jackson, 1996; Ruiz Cruz and Novak, 2003).

In contrast, Na substitution in dioctahedral micas is extensive and the paragonite+muscovite (or phengite) assemblage is common in metamorphosed pelites and basic rocks. Even though the existence of a miscibility gap in the muscovite–paragonite system has been well documented (Deer *et al*., 1976; Guidotti, 1984), apparent intermediate compositions between muscovite and paragonite have also been described. These intermediate compositions have been interpreted as due to the presence of very fine-scale intergrowths of paragonite and muscovite (*e.g*. Shau *et al*., 1991), mixed-layer paragonite-muscovite (*e.g*. Frey, 1969) or homogeneous metastable solid-solution of muscovite and paragonite (*e.g*. Livi *et al*., 1988; Jiang and Peacor, 1993).

* E-mail address of corresponding author:
mdruiz@uma.es
DOI: 10.1346/CCMN.2004.0520506

Sodium and intermediate Na-K biotite packets coexisting with K biotite have recently been identified in a schist from the Maláguide Complex (Betic Cordilleras, Spain). The micas offer wide variations in Na and K contents, ranging from typical K biotite to Na biotite. The complex intergrowths of these micas have been characterized using X-ray diffraction (XRD), electron microprobe (EMPA), scanning (SEM) and transmission-analytical electron microscopy (TEM/AEM).

EXPERIMENTAL TECHNIQUES

X-ray diffraction patterns were recorded using a Siemens D-5000 diffractometer with CuKα radiation and graphite monochromator, operated at 40 mA and 40 kV with a 0.01º2θ step size and 2 s counting time. Randomly oriented samples were used for determination of semi-quantitative mineral compositions (Shultz, 1964). Oriented samples, obtained in the air-dried state (natural and Mg-saturated samples), after ethylene glycol solvation (EG) and after heating at 500ºC, were used for the identification of phyllosilicates. Quartz was used as an internal standard.

Polished and carbon-coated thin-sections were investigated by EMPA, using a Cameca SX-50 instrument. The ZAF corrections and data reductions were performed with the software package supplied by Cameca. The EMPA data were collected using an accelerating voltage of 20 kV, a beam current of 20 nA and a beam size of 5 µm, in order to minimize evaporation of the light elements. Under routine operating conditions, the accuracy is ~1.5% of the measured concentrations. Standards were wollastonite (Si and Ca), synthetic Al_2O_3 (Al), orthoclase (K), albite (Na), synthetic Fe_2O_3 (Fe), periclase (Mg) and synthetic $MnTiO_3$ (Mn and Ti). Thin-sections were also studied by SEM, using a JEOL JSM-6400 instrument, equipped with an OXFORD (Link-Pentafet) analyzer.

Slices were removed from petrographic thin-sections and thinned to electron transparency by argon ion-milling, using a GATAN Duomill 600. An initial beam tilt of 15º and 1 mA were used until the sample was perforated, and the current was lowered to 0.6 mA for 1 h. Final cleaning was carried out at 12º and 0.4 mA. Specimens were coated with carbon and examined using a Philips CM-20 transmission electron microscope (TEM), operating at 200 kV, equipped with an EDAX energy-dispersive X-ray solid-state (EDX) detector (ultrathin window). Scanning TEM mode was used for quantitative analyses (AEM) of particles using a 40 Å diameter beam and variable scanning area, according to the packet size. Muscovite, albite, spessartine, olivine and titanite were used as standards to calculate K factors by the thin-film method of Lorimer and Cliff (1976). Under routine operating conditions, accuracy is ~3% of the measured concentrations for all elements except for the lighter ones ($\approx$8%).

RESULTS

Occurrence and petrography

The Internal zones of the Betic Cordilleras (Spain) comprise three main tectonic complexes: The Nevado-Filábride, the Alpujárride and the Maláguide, with decreasing metamorphic grade (Egeler and Simon, 1969). The distinction between the Maláguide and the Alpujárride rocks is based on both lithology and metamorphic grade. Differentiation between the two complexes is easy in Triassic and upper Paleozoic terrains but the deepest Paleozoic schists are very similar in both complexes. As a consequence, materials with uncertain provenance have been included, in the Málaga area, within the 'intermediate' Benamocarra unit. The sample described in this work was collected from the Ordovician-to-Silurian schists of this intermediate unit, ~10 km northeast of Málaga (Figure 1).

The mineralogy of the schists is characterized by the association quartz + albite + muscovite + biotite + garnet ± andalusite ± staurolite, typical of the amphibolite facies. The sample described here shows the assemblage quartz + albite + muscovite + biotite + garnet + andalusite. Approximate mineral abundance, deduced from the XRD patterns, are: quartz 35%; plagioclase 10%; micas 46%; andalusite 6%; garnet 3%, together with minor accessory phases (ilmenite, zircon, Fe oxides). Biotite, muscovite and large andalusite porphyroblasts are parallel to the main schistosity, although biotite grains with other orientations are also present (Figure 2). Garnets display marginal alteration to Fe oxides, whereas biotite grains show scarce alteration to kaolinite, only evident in backscattered electron (BSE) images (Figure 3). Alteration is located at the oblique interfaces between biotite and muscovite, suggesting that these interfaces were favorable to circulation of fluids.

X-ray diffraction data

The XRD patterns of the bulk biotite-bearing schists are characterized by the presence of an intense 10 Å reflection frequently displaying small associated reflections at 14 and 7 Å (Figure 4). The form of the reflections does not change after ethylene glycol solvation, whereas heating at 500ºC causes the disappearance of the 14 Å reflection and a sharpening and increase in intensity of the 10 Å reflection. The 7 Å reflection remains unchanged. This behavior indicates the presence of minor vermiculite-like phases (hydrated biotite) and kaolinite together with the dominant micas (Brown and Brindley, 1980). Diffraction peaks observed at ~2 and 1.956 Å suggest the presence of a small amount of a Na biotite together with muscovite and K biotite (Figure 5). This is consistent with the lower basal spacing observed for Na-rich trioctahedral phases (Spear *et al.*, 1981). This phase has been identified by TEM/AEM (see below).

https://doi.org/10.1346/CCMN.2004.0520506 Published online by Cambridge University Press

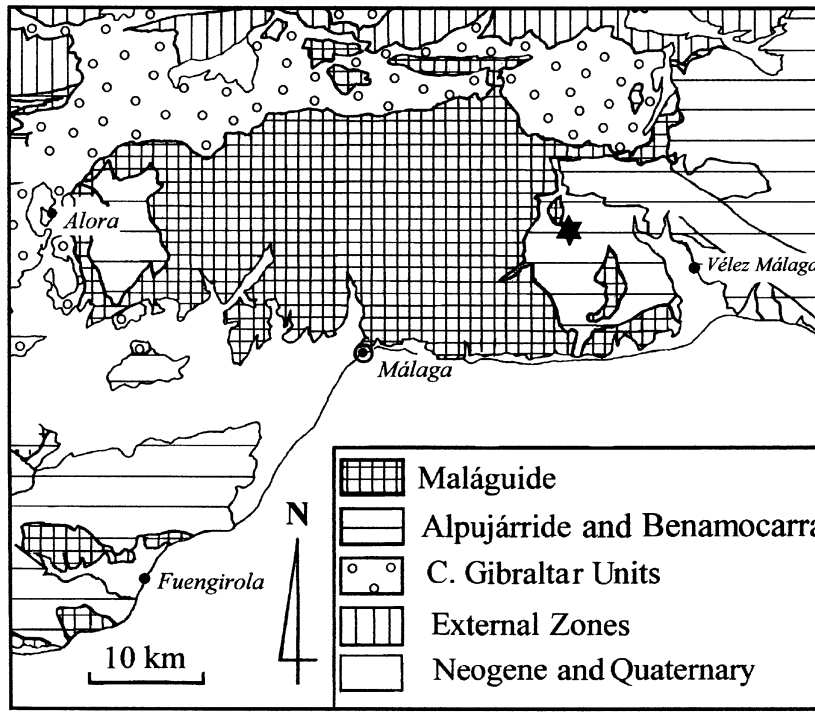

Figure 1. Sketch map of the Málaga area showing the distribution of the Maláguide and Alpujárride complexes and the location of the sample studied (star). Modified from IGME (1987).

Electron microprobe data

The EMPA study did not reveal the presence of biotite with anomalous Na contents. Indeed, EMPA results for of biotite (Table 1) are very homogeneous and show low Na contents (on the order of 0.02 atoms per 11 oxygens). The measured Ti content is characteristic of metamorphic biotite (Guidotti, 1984). Biotite analyses are also characterized by low totals (on the order of 90%) and by a slight deficit of interlayer charge. Both features are quite common for microprobe analyses of trioctahedral micas (Deer *et al*., 1976), and especially in Na-bearing micas, and suggest the presence of H_3O^+ replacing interlayer cations.

Coexisting phases have also been analyzed by EMPA (Table 1). Sodic plagioclase shows compositions ranging from albite to sodic oligoclase. The composition of the muscovite grains is homogeneous. The ^{IV}Si content is on the order of 3.10–3.17 atoms per formula unit (a.p.f.u., also calculated for 11 oxygens) and the total interlayer charge ranges from 0.86 to 0.97, the Na content being on the order of 0.10 a.p.f.u. The Fe+Mn+Mg content is as high as 0.65 a.p.f.u. The

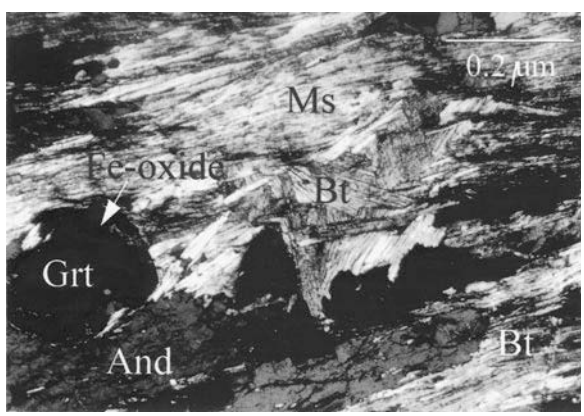

Figure 2. Polarized-light micrograph showing the mineral assemblage in the schist studied. Ms: muscovite. Bt: biotite. And: andalusite. Grt: garnet.

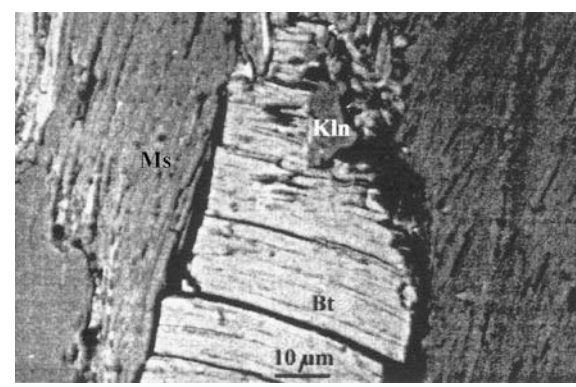

Figure 3. Backscattered image showing the incipient alteration of biotite (Bt) to kaolinite (Kln). This alteration is only observed at the inclined interfaces between biotite and muscovite (Ms).

https://doi.org/10.1346/CCMN.2004.0520506 Published online by Cambridge University Press

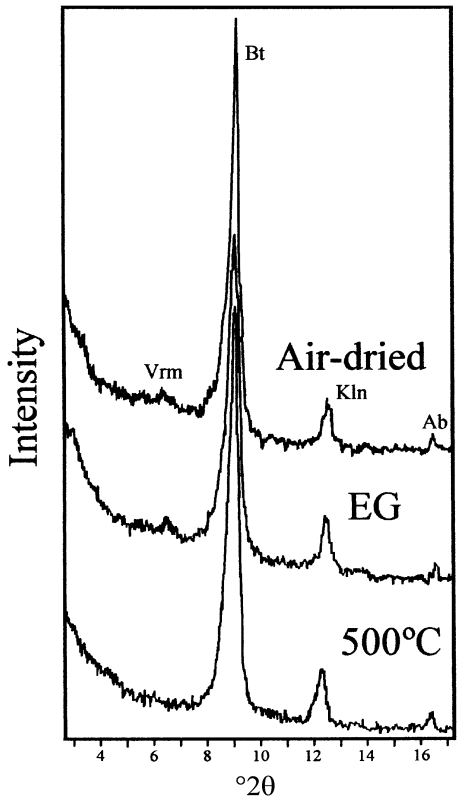

Figure 4. XRD patterns obtained from oriented samples of the 2−20 μm size fraction of the schist in the air-dried state, after EG treatment and after heating at 500ºC. Bt: biotite. Ms: muscovite. Kln: kaolinite. Vrm: vermiculite. Ab: albite.

garnets are also compositionally homogeneous, being almandine-rich varieties, with Ca contents on the order of 0.50 a.p.f.u. (for 12 oxygens), and Mn contents <0.10 a.p.f.u.. The andalusite contains a limited amount of Fe (up to 0.3 a.p.f.u. for 5 oxygens).

Transmission and analytical electron microscope study

Aggregates of micas similar to those shown in Figure 2 were studied by TEM/AEM. This study revealed the presence of fine intergrowths of tri-octahedral micas, with variable Na/K ratios. Figure 6 shows a low-magnification TEM image of coexisting K biotite, Na biotite and intermediate Na-K biotite, with parallel or subparallel basal planes. The interfaces are also parallel to the basal planes of one or both of the adjacent micas.

Potassium biotite commonly occurs as stacks of parallel packets, with thickness on the order of microns. The lattice fringe images show a regular 10 Å periodicity, a characteristic mottled aspect, and few structural defects, mainly consisting of rectangular or lenticular zones that appear light in TEM images (Figure 7), probably due to electron beam damage of hydrated interlayers. In spite of the lower accuracy of the AEM data relative to the EMPA data, the AEM data reveal compositional variability within the K biotite packets that were not detected by EMPA (Table 2). According to the AEM data, the tetrahedral Si content ranges from 2.78 to 2.93 a.p.f.u., and the octahedral occupancy between 2.78 and 2.93 a.p.f.u. Potasssium biotite is also characterized by the presence of Ti (up to 0.12 a.p.f.u.). In addition, the total interlayer charge (0.85−0.90) is greater than that determined by EMPA. The Fe/(Fe+Mg) ratio is, however, homogeneous, of the order of 0.50.

In some regions, the biotite packets appear retrograded to kaolinite-like phases. These appear as small, randomly oriented rectangular packets and as spherical particles (Figure 8) with a composition similar to that of kaolinite and which probably correspond to halloysite.

Sodium-rich biotite forms packets with variable thickness. The lattice images show straight fringes with a regular ~10 Å spacing and high concentrations of structural defects; these occur mainly at terminal regions of 5.8 Å fringes and probably correspond to brucite-like sheets (Figure 9). The wavy character of unequally contracted vermiculite layers (*e.g.* Ruiz Cruz, 1999) was not observed in these packets. The AEM data (Table 2) revealed notable differences between Na- and K-bearing packets, which cannot be explained solely on

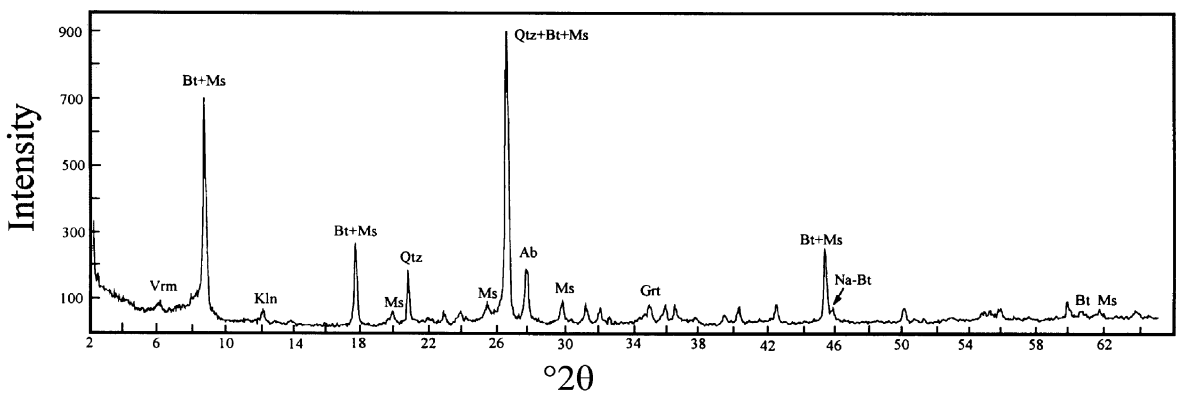

Figure 5. XRD pattern obtained in the range 2−65º2θ, from an oriented sample. The ~2 Å reflections at ~45.5º2θ reveals the presence of Na-rich phases. Qtz: quartz, Ab: albite, Grt: garnet, Bt: biotite, Ms: muscovite, Kln: kaolinite, Vrm: vermiculite.

https://doi.org/10.1346/CCMN.2004.0520506 Published online by Cambridge University Press

Table 1. Significant EMPA analyses of minerals coexsisting in the Na biotite-bearing schist.

	Ms	Bt	Bt	Bt		Pl	And	Grt
SiO_2	46.444	37.256	36.857	36.232		63.819	36.241	36.901
Al_2O_3	35.797	20.367	19.628	19.705		22.228	62.638	20.830
TiO_2	0.374	2.189	2.012	2.346		0.000	0.000	0.130
Cr_2O_3	0.025	0.041	0.044	0.033		0.000	0.026	0.000
FeO	0.863	15.637	17.331	16.422		0.000	0.240	24.226
MnO	0.000	0.163	0.201	0.160		0.026	0.000	10.084
MgO	0.588	8.025	7.862	7.353		0.001	0.046	0.833
CaO	0.052	0.143	0.328	0.438		3.195	0.005	5.995
Na_2O	0.667	0.097	0.134	0.145		9.767	0.007	0.027
K_2O	9.550	7.702	7.110	6.524		0.281	0.001	0.002
Total	94.370	91.622	91.505	89.357		99.318	99.240	99.029
Si	3.09	2.84	2.84	2.85	Si	2.83	0.99	3.01
^{IV}Al	0.91	1.16	1.16	1.15	Al	1.16	2.01	2.00
^{VI}Al	1.89	0.67	0.71	0.67	Fe	0.00	0.01	1.65
Ti	0.02	0.13	0.12	0.14	Mn	0.00	0.00	0.70
Fe	0.05	1.00	1.12	1.08	Mg	0.00	0.00	0.10
Mn	0.00	0.01	0.01	0.01	Ca	0.15	0.00	0.52
Mg	0.06	0.91	0.90	0.86	Na	0.84	0.00	0.00
Ca	0.00	0.01	0.03	0.04	K	0.02	0.00	0.00
Na	0.09	0.01	0.02	0.02				
K	0.81	0.75	0.70	0.65				
O	11	11	11	11		8	5	12

Ms: muscovite, Bt: biotite, Pl: plagioclase, And: andalusite, Grt: garnet

the basis of a Na substitution for K. Specifically, the tetrahedral Si contents are systematically >3 a.p.f.u.. Similar Si contents characterize wonesite (Spear *et al*., 1981). The octahedral occupancy is lower than that determined in K biotite. Other differences are the lack of Ti, the higher Ca content and the Fe/(Fe+Mg) ratio (of the order of 0.80), which is notably higher than in K-bearing packets.

In addition, a third type of mica phase was identified having similar Na and K contents. This phase is very similar to the K-rich phase, although it shows a higher concentration of beam-damaged areas (Figure 10). The chemical composition of these packets (Table 2) is intermediate between the K-rich and Na-rich biotite, and it was variable even within a single packet, revealing the presence of microdomains enriched either in Na or in K.

The selected area electron diffraction patterns (SAED) viewed along [100] or [110] show some differences among the three chemically different phases (Figure 11). The diffraction patterns of K- and intermediate Na-K biotite exhibit well-defined ~30 Å reflections in the 0*kl* reflection rows with $k \neq 3n$. This periodicity suggests the presence of a three-layer mica polytype.

In contrast, the SAED patterns of Na-rich packets reveal abundant stacking disorder, as indicated by the streaking within 0*kl* reflection rows. In addition, a

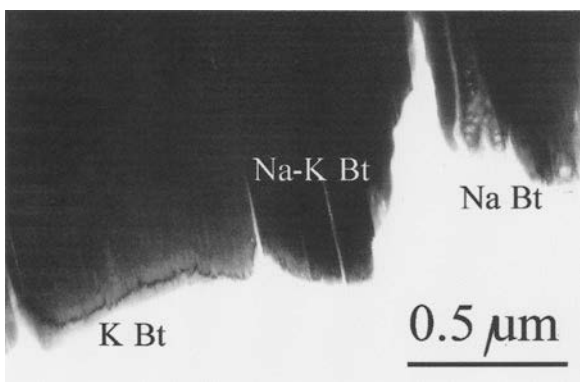

Figure 6. Low-magnification TEM image showing an intergrowth of K biotite (K Bt), intermediate Na-K biotite (Na-K Bt) and Na biotite (Na Bt).

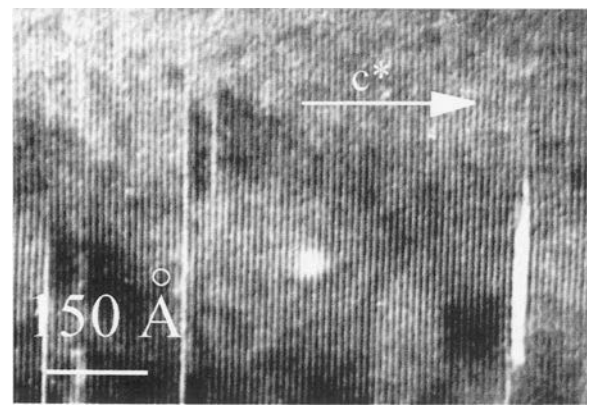

Figure 7. HRTEM image of a K biotite packet showing regular 10 Å periodicity and the presence of lenticular light gaps, corresponding to damaged areas.

https://doi.org/10.1346/CCMN.2004.0520506 Published online by Cambridge University Press

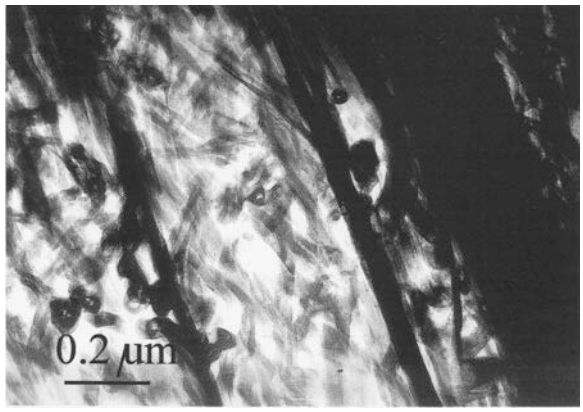

Figure 8. Low-magnification TEM image showing the alteration of K biotite to randomly oriented small packets and spheres of probable halloysite.

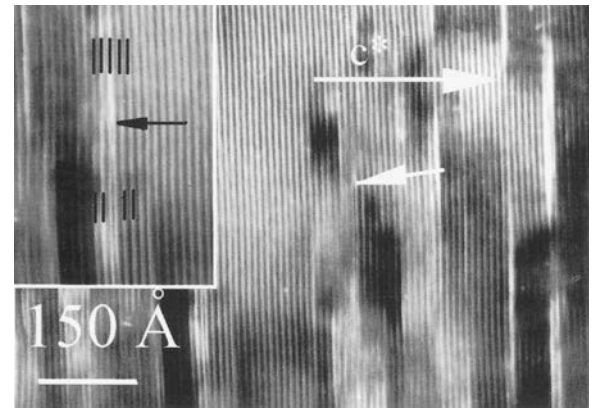

Figure 9. HRTEM image of Na biotite. The ~10 Å layers are intergrown with terminal 5.8 Å layers (arrowed), probably corresponding to brucite-like sheets.

comparison of the SAED patterns of the three phases reveals a decrease in the basal spacing from 10.1 Å in the case of the K-rich phase, to 9.78 Å in the case of the Na-rich phase. Regions with intermediate compositions show intermediate basal spacings.

Textural relations among Na biotite and other metamorphic phases

Neither optical examination nor EMPA data have permitted the identification of the Na-rich phase, due to the fact that it always occurs as submicroscopic intergrowths within the more abundant K-rich phase. With the aim of determining the textural relationships among Na biotite and intermediate biotites and the other metamorphic phases, a SEM study was also carried out. In comparison with EMPA, the SEM permits the rapid analysis of a greater number of grains or areas within a single grain, thus facilitating the identification of the Na-rich packets. As with EMPA, SEM examination showed that the Na content is, in most biotite grains, below the detection level. Although microscopic grains of Na biotite were not identified by SEM, a notable enrichment in Na was observed in biotite grains in some microdomains associated with albite grains. In these areas, Na/K ratios of the order of 0.5 were measured in biotite (Figure 12). Moreover, small albite grains appear included and partially replaced by biotite (Figure 13), suggesting that growth of Na biotite consumed albite.

DISCUSSION

The structural nature of the Na trioctahedral micas

There are few reports of naturally occurring Na-rich trioctahedral micas. In addition, the different phases described in previous studies show marked differences in the interlayer occupancy and amount of Tschermaks substitution ($Al_2Mg_{-1}Si_{-1}$), suggesting that a wide range of chemical variability is possible in Na trioctahedral micas.

Sodium phlogopite (Schreyer *et al*., 1980) or aspidolite (according to the recent mica nomenclature by Rieder *et al*., 1998) has a composition near the ideal $NaMg_3(AlSi_3)O_{10}(OH)_2$, with little Tschermaks substitution and few interlayer vacancies. In contrast, the Al-rich phase preiswerkite (Keusen and Peters, 1980), with composition near $NaMg_2Al(Al_2Si_2)O_{10}(OH)_2$, shows

Table 2. Representative AEM data for K biotite, Na biotite and K-Na biotite (formulae calculated for $O_{10}(OH)_2$).

	K Bt 1	K Bt 2	K Bt 3	K Bt 4	Na Bt 5	Na Bt 6	Na Bt 7	K-Na Bt 8	K-Na Bt 9	K-Na Bt 10	K-Na Bt 11
Si	2.93	2.85	2.78	2.78	3.23	3.21	3.24	3.03	2.70	2.86	2.77
^{IV}Al	1.07	1.15	1.22	1.22	0.77	0.79	0.76	0.97	1.30	1.14	1.23
^{VI}Al	0.71	0.67	0.54	0.61	0.91	0.77	0.81	0.85	0.54	0.65	0.23
Ti	0.10	0.12	0.04	0.05	0.00	0.00	0.01	0.05	0.00	0.03	0.00
Fe	0.86	0.90	1.11	1.03	1.09	1.52	1.43	1.22	1.45	1.08	2.40
Mg	0.96	0.95	1.13	1.05	0.37	0.25	0.29	0.99	0.85	1.02	0.43
Ca	0.03	0.07	0.09	0.05	0.18	0.14	0.15	0.04	0.05	0.05	0.06
Na	0.16	0.14	0.12	0.17	0.57	0.45	0.45	0.27	0.52	0.48	0.44
K	0.71	0.65	0.73	0.63	0.18	0.20	0.11	0.64	0.49	0.43	0.34
Fe/(Fe+Mg)	0.47	0.49	0.50	0.50	0.75	0.86	0.83	0.55	0.63	0.51	0.85

https://doi.org/10.1346/CCMN.2004.0520506 Published online by Cambridge University Press

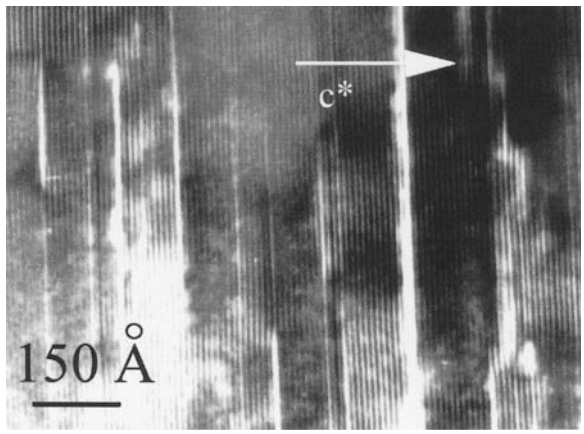

Figure 10. HRTEM image of the intermediate Na-K biotite shows regular ~10 Å fringes with abundant light, damaged areas.

fully occupied interlayer sites and almost complete Tschermaks substitution. Wonesite (Spear *et al*., 1981; Veblen, 1983) has some Fe and a composition near $(Na,K)_{0.5}Mg_{2.2}Fe_{0.4}Al_{0.3}(Al_{0.8}Si_{3.2})O_{10}(OH)_2$, with a larger proportion of interlayer vacancies and a significant degree of Tschermak's substitution.

Typical Fe-bearing biotites, such as those described by Dempster and Jackson (1996), show a mean composition $(Na,K)_{0.6}Mg_{0.9}Fe_{1.4}Al_{0.4}(Al_{1.3}Si_{2.7})O_{10}(OH)_2$ and also have a large proportion of interlayer vacancies but with lower Si contents than wonesite. The Na-rich hydrated biotites described by Ruiz Cruz and Novak (2003) show a mean composition of $(Ca,Na,K)_{0.75}Mg_{1.1}Fe_{1.5}Al_{0.5}(Al_{1.6}Si_{2.4})O_{10}(OH)_2$, very similar to Na biotites described by Dempster and Jackson (1996), but with relatively high interlayer charge.

In addition to chemical variability, Na-rich trioctahedral micas show different degrees of expansion in water or ethylene glycol, the expansion probably being favored by low interlayer charge. In most cases the basal spacing determined in the air-dried state is typical of micas (near 10 Å) although some other phases (*e.g.* those described by Ruiz Cruz and Novak, 2003) show a basal spacing of 14 Å, similar to vermiculite, although they do not expand with ethylene glycol. Thus, the H_3O^+ content in Na trioctahedral micas appears to be very variable. According to Carman (1974), low-temperature hydration of Na trioctahedral micas seems to preclude the occurrence of these phases in natural rocks. Indeed it is possible, as suggested by Schreyer *et al*. (1980), that many vermiculites interpreted as weathering or retrograde products of biotite, in fact represent hydrated forms of Na trioctahedral phases.

Both the chemical composition of our micas and their behavior after glycolation agree with these observations. The biotites described in this study show relatively high interlayer charge in comparison with the more usual Na-rich micas, and hydration appears to be very limited, as

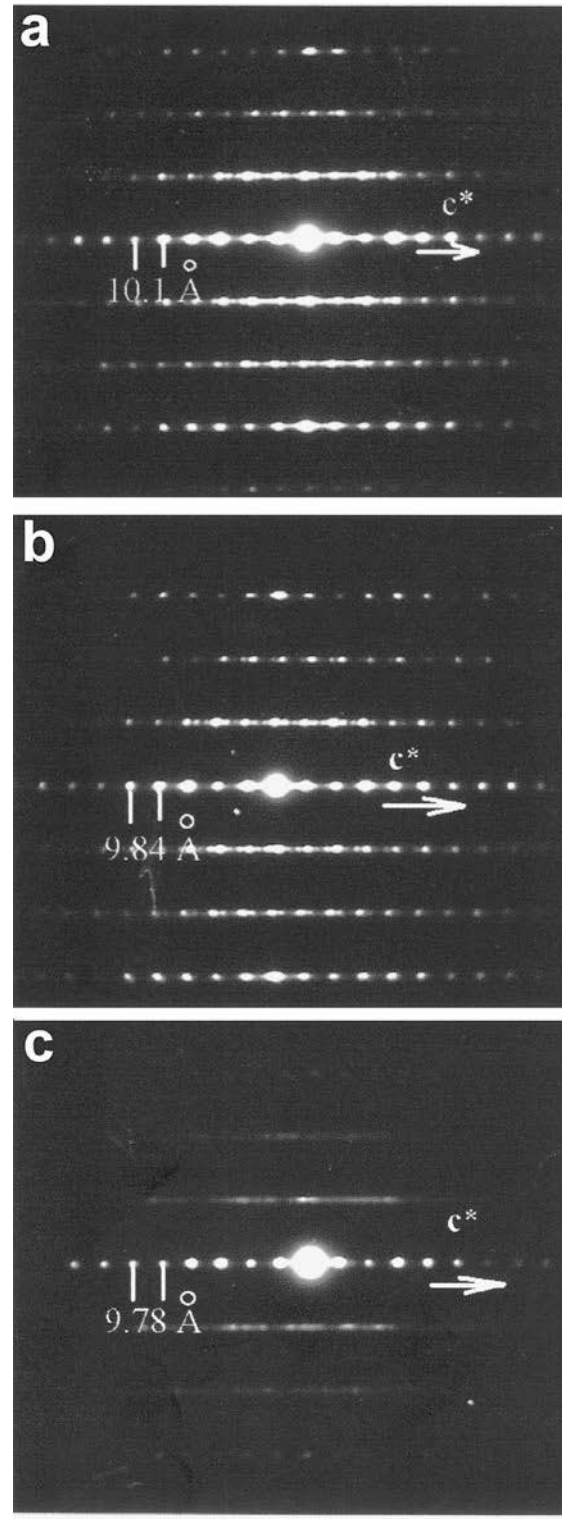

Figure 11. SAED patterns viewed along the 100/110 zone axis of the K biotite (K Bt) (a), the intermediate Na-K biotite (Na-K Bt) (b) and the Na-rich biotite (Na Bt) (c), showing the decreasing basal spacing with the increase in Na content. The distances indicated on the SAED patterns are the real-space equivalents of the reciprocal lattice spacings.

https://doi.org/10.1346/CCMN.2004.0520506 Published online by Cambridge University Press

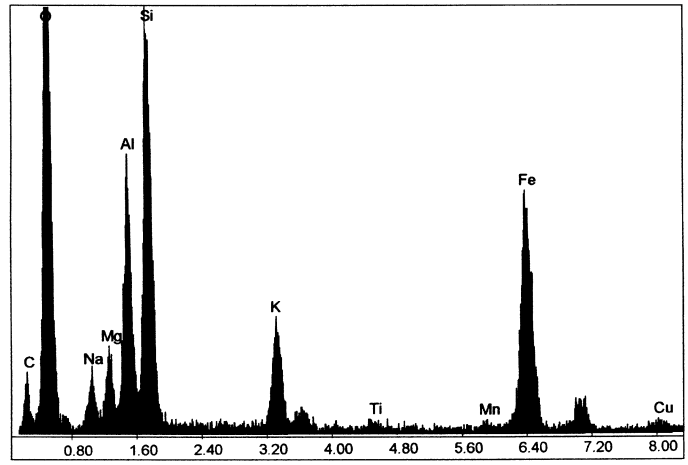

Figure 12. X-ray spectra (SEM) of the Na-enriched biotite grains, located in plagioclase-rich microdomains.

indicated by the low vermiculite content. Likewise, the degree of expansion in the presence of ethylene glycol is nil, as observed in Figure 4.

The intermediate Na-K biotite described here poses the problem of whether this material represents one or two phases, as in the case of white micas (see Jiang and Peacor, 1993). It is very difficult to prove that the intermediate phases do not comprise two phases below the analytical resolution of the TEM. Nevertheless, the intermediate Na-K biotite occurs as thick stacks of layers (in the order of several hundred Å) that give only one set of 00*l* reflections, with a 9.84 Å periodicity in electron diffraction patterns (see Figure 11), suggesting that they are in fact a single phase.

The origin of the Na biotites in the Betic schists

The Na-rich and intermediate Na-K di- and trioctahedral micas described in previous studies have systematically been found in metamorphic terrains. Some of these phases (*e.g.* wonesite) have been interpreted as having formed through prograde metamorphism whereas other occurrences have been viewed as a result of hydrothermal alteration. Thus, the formation of Na-rich and intermediate Na-K dioctahedral micas in metavolcanics has been related by Jiang and Peacor (1993) to the existence of a hydrothermal event which would supply the necessary Na and K from the adjacent pelites. In a similar way, Dempster and Jackson (1996) explain the formation of Na-rich biotite through the interaction of hydrothermal Na-rich fluids with pre-existing K biotite. In these cases, both the textural relations and the chemical composition of the K- and Na-rich micas support these interpretations.

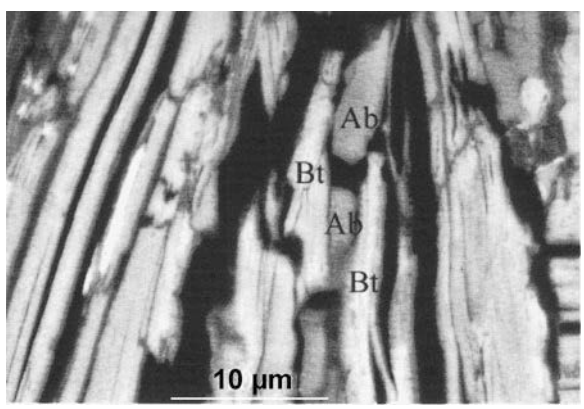

Figure 13. BSE image showing small slabs of albite, partially replaced by Na-enriched biotite grains. Ab: albite, Bt: biotite.

In the case of the Betic Cordilleras micas, however, there is no evidence of a hydrothermal event, and most of the phases coexisting with Na biotite (*e.g.* muscovite) are not enriched in Na (Table 1). A generalized retrogression of K biotite to Na-rich phases can also be discounted, since the retrograde alteration of biotite is rare, is localized to the rims of biotite grains, and results in the precipitation of kaolin minerals (Figure 3). Moreover, both muscovite and biotite crystals follow the main schistosity (Figure 2), suggesting that these grew during a common prograde Alpine metamorphic episode. On the other hand, the study of the Maláguide metaclastites at the regional scale indicates that Na-rich trioctahedral phases (mixed-layer mica-chlorite and chlorite-vermiculite) are common constituents of the metamorphic assemblage of these rocks (Ruiz Cruz, 1999, 2001; Ruiz Cruz and Novak, 2003). Thus, the origin of Na biotite and intermediate Na-K biotite must represent a higher metamorphic grade than that responsible for the formation of 'vermiculitic phases' in the overlying Paleozoic sequence.

Most of the reactions proposed for biotite formation at low-grade conditions consume chlorite, the most frequently cited (Yardley, 1989; Miyashiro, 1994) being

$$\text{phengite} + \text{chlorite} = \text{biotite} + \text{muscovite} + H_2O \quad (1)$$

and

https://doi.org/10.1346/CCMN.2004.0520506 Published online by Cambridge University Press

K-feldspar + chlorite =
biotite + muscovite + quartz + H_2O (2)

which take place at ~400ºC, at intermediate pressures.

In the case of the Maláguide complex, lack of K-feldspar in the underlying sequence suggests that reaction 1 was responsible for most K biotite formation. Nevertheless, the presence of both Na and K micas and the textural evidence (see Figure 13) suggest that two parallel reactions involving, chlorite + phengite and chlorite + albite, respectively, must be responsible for the formation of these intergrowths. The reaction

Na-feldspar + chlorite = Na biotite + quartz + H_2O (3)

is proposed for the formation of Na biotite. A higher grade of metamorphism would probably be necessary to homogenize the composition of the biotite grains.

CONCLUSIONS

Sodium biotite and Na-K biotite intergrown with more abundant K biotite have been identified in a deep Paleozoic schist from the Maláguide Complex. The TEM data show that both Na and Na-K biotites occur as chemically homogeneous stacks of layers that give only one set of 00*l* reflections, with 9.78 and 9.84 Å, respectively, in the SAED patterns, whereas mixed layering was not observed. Only the 005 (or 00,10) reflection of micas (at ~2.00 Å) appears as a double peak, in the XRD pattern, revealing the presence of Na biotite.

The formation of Na, Na-K and K biotite occurred during prograde Alpine metamorphism, according to the available data. The crystallization of Na biotite reflects a metamorphic grade higher than that responsible for the formation of Na-rich 'vermiculitic phases' in the overlying Paleozoic sequence. These phases seldom form micron-scale grains, and their identification is only possible by TEM/AEM. In addition, low-temperature hydration of these phases is very easy, producing vermiculite. Therefore, the possibility that Na-rich phases similar to those described here might be common in metamorphic terrains cannot be discarded.

ACKNOWLEDGMENTS

The author is grateful to K.J.T. Livi, P.J. Heaney and H. Konishi, whose corrections and suggestions have notably improved the manuscript. Thanks also to A. Gómez and M.M. Abad for their help in obtaining the TEM/AEM data. This study received financial support from the Project BTE-2000-1150 (Ministerio de Educación y Cultura) and from the Research Group RNM-199.

REFERENCES

Brown, G. and Brindley, G.W. (1980) X-ray procedures for clay mineral identification. Pp. 305–360 in: *Crystal Structures of Clay Minerals and their X-ray Identification* (G.W. Brindley and G. Brown, editors). Monograph **5**, Mineralogical Society, London.

Cabella, R., Gazzotti, M. and Luccetti, G. (1997) Loveringite and baddeleyite in layers of chromian spinel from the Bracco ophiolitic unit, northern Apennines, Italy. *The Canadian Mineralogist*, **35**, 899–908.

Carman, J.H. (1974) Synthetic sodium phlogopite and its two hydrates: stabilities, properties, and mineralogic implications. *American Mineralogist*, **59**, 261–273.

Deer, W.A., Howie, R.A. and Zussman, J. (1976) *Rock Forming Minerals. Sheet Silicates*. Longman, London, 270 pp.

Dempster, T.J. and Jackson, R.A. (1996) Na-biotite in Dalradian pelitic schists, Angus. *Scottish Journal of Geology*, **32**, 173–177.

Egeler, C.G. and Simon, O.J. (1969) Orogenic evolution of the Betic Zone (Betic Cordilleras, Spain), with emphasis on the nappe structures. *Geologie en Mijnbouw*, **48**, 296–305.

Frey, M. (1969) A mixed-layer paragonite/phengite of low-grade metamorphic origin. *Contributions to Mineralogy and Petrology*, **24**, 63–65.

Godard, G. and Smith, D.C. (1999) Preiswerkite and Na-(Mg,Fe)-margarite in eclogites. *Contributions to Mineralogy and Petrology*, **136**, 20–32.

Guidotti, C.V. (1984) Micas in metamorphic rocks. Pp. 357–368 in: *Micas* (S.W. Bailey editor). Reviews in Mineralogy, **13**. Mineralogical Society of America, Washington D.C.

IGME (1987) *Mapa geológico de España (1:50000) Hoja de Málaga (1053)*. Centro de Publicaciones del Ministerio de Industria y Energía, Madrid.

Jiang, W.T. and Peacor, D.R. (1993) Formation and modification of metastable intermediate sodium potassium mica, paragonite, and muscovite in hydrothermally altered metabasites from northern Wales. *American Mineralogist*, **78**, 782–793.

Keusen, H.R. and Peters, Tj. (1980) Preiswerkite, an Al-rich trioctahedral sodium mica from the Geisspfad ultramafic complex (Penninic Alps). *American Mineralogist*, **65**, 1134–1137.

Livi, K.J.T., Veblen, D.R. and Ferry, J.M. (1988) Electron microscope study of anchizone and epizone metamorphosed shales from the central Swiss Alps. *Geological Society of America, Abstracts with Programs*, **20**, A244.

Lorimer, G.W. and Cliff, G. (1976) Analytical electron microscopy of minerals. Pp. 506–519 in: *Electron Microscopy in Mineralogy* (H.R. Wenk editor). Springer-Verlag, New York.

Melcher, F., Grum, W., Simon, G., Thalhammer, T.V. and Stumpfl, E.F. (1997) Petrogenesis of the ophiolitic giant chromite deposits of Kempirsai, Kazakhstan: a study of solid and fluid inclusions in chromite. *Journal of Petrology*, **38**, 1419–1458.

Meyer, J. (1983) The development of the high-pressure metamorphism in the Allalin metagabbro (Switzerland). High-pressure metamorphism: indicator of subduction and crustal thickening (abstract). *Terra Cognita*, **3**, 187.

Miyashiro, A. (1994) *Metamorphic Petrology*. UCL Press, London, 404 pp.

Peng, G.Y., Lewis, J., Lipin, B., McGee, J., Bao, P.S. and Wang, X.B. (1995) Inclusions of phlogopite and phlogopite hydrates in chromite from the Hongguleleng ophiolite in Xinjiang, northwest China. *American Mineralogist,* **80**, 1307–1316.

Rieder, M., Cavazzini, G., D'yakonov, Y.S., Frank-Kamenetskii, V.A., Gottardi, G., Guggenheim, S., Koval, P.V., Müller, G., Neiva, A.M.R., Radoslovich, E.W., Robert, J.L., Sassi, F.P., Takeda, H., Weiss, Z. and Wones, D.R. (1998) Nomenclature of the micas. *Clays and Clay Minerals*, **46**, 586–595.

Ruiz Cruz, M.D. (1999) New data for metamorphic vermiculite. *European Journal of Mineralogy*, **11**, 533–548.

Ruiz Cruz, M.D. (2001) Mixed-layer mica-chlorite in very low-grade metaclastites from the Maláguide Complex (Betic Cordilleras, Spain). *Clay Minerals*, **36**, 307–324.

Ruiz Cruz, M.D. and Novak, J. (2003) Metamorphic chlorite and 'vermiculitic' phases in mafic dikes from the Maláguide Complex (Betic Cordillera, Spain). *European Journal of Mineralogy*, **15**, 67–80.

Schreyer, W., Abraham, K. and Kulke, H. (1980) Natural sodium phlogopite coexisting with potassium phlogopite and sodium aluminium talc in a metamorphic evaporite sequence from Derrag, Tell Atlas, Algeria. *Contributions to Mineralogy and Petrology*, **74**, 223–233.

Shau, Y.-H., Feather, M.E., Essene, E.J. and Peacor, D.R. (1991) Genesis and solvus relations of submicroscopically intergrown paragonite and phengite in a blueschist from northern California. *Contributions to Mineralogy and Petrology*, **106**, 367–378.

Shultz, L.G. (1964) Quantitative interpretation of mineralogical composition from X-ray and chemical data for the Pierre Shale. *US Geological Survey Professional Paper*, **391-C**, 31 pp.

Smith, D.C. (1988) A review of the peculiar mineralogy of the 'Norwegian coesite-eclogite province', with crystal-chemical, petrological, geochemical and geodynamical notes and extensive bibliography. Pp. 1–206 in: *Eclogites and Eclogite-facies Rocks* (D.C. Smith, editor). Elsevier, Amsterdam.

Spear, F.S., Hazen, R.M. and Rumble, D. (1981) Wonesite: a new rock-forming silicate from the Post Pond Volcanics, Vermont. *American Mineralogist*, **66**, 100–105.

Veblen, D.R. (1983) Exsolution and crystal chemistry of the sodium mica wonesite. *American Mineralogist*, **68**, 554–565.

Yang, J.J. and Jahn, B.M. (2000) Deep subduction of mantle-derived garnet peridotites from the Su-Lu UHP metamorphic terrane in China. *Journal of Metamorphic Geology*, **18**, 167–180.

Yardley, B.W.D. (1989) *An Introduction to Metamorphic Petrology*. Longman, Essex, England, 248 pp.

(*Received 29 September 2003; revised 10 May 2004; Ms. 840; A.E. Peter J. Heaney*)